Journal of Materials Chemistry C

PAPER

View Article Online
View Journal | View Issue

Spin crossover composite materials for electrothermomechanical actuators†

Cite this: J. Mater. Chem. C, 2014, 2, 2949

Il'ya A. Gural'skiy,[ab] Carlos M. Quintero,[c] José Sánchez Costa,[a] Philippe Demont,[d] Gábor Molnár,[a] Lionel Salmon,[a] Helena J. Shepherd*[e] and Azzedine Bousseksou*[a]

Received 10th February 2014
Accepted 2nd March 2014

DOI: 10.1039/c4tc00267a

www.rsc.org/MaterialsC

Composites of the spin crossover complex $[Fe(trz)(H\text{-}trz)_2](BF_4)$ (H-trz = 1,2,4-4*H*-triazole and trz = 1,2,4-triazolato) dispersed in a poly(methylmethacrylate) (PMMA) matrix were synthesized and investigated for their spin crossover properties by optical reflectivity, Raman spectroscopy and calorimetry. These composite films were used to fabricate bilayer cantilevers that can perform efficient and tuneable mechanical actuation based on the spin transition. A prototype device that uses the spin transition phenomenon to convert electrical energy into mechanical motion through Joule heating is described. This device is used to perform oscillatory actuation driven by a modulated current. The ability to tune the performance of this electromechanical system is demonstrated by varying the working temperature, the applied ac current and its frequency.

Introduction

The transformation of electrical energy into motion is one of the main demands from micro- and nanoelectromechanical systems (MEMS and NEMS).[1] This conversion could be achieved *via* electrostatic[2] or piezoelectric effects,[3] Joule heating,[4] *etc.* Among these methods electrothermal actuation is a widely used approach due to its simplicity both for the fabrication process and the actuation mechanism.[5] The choice of the actuating material is a crucial step in the construction of a new electromechanical system and the numerous specific requirements make the development of novel actuating materials necessary.[6] For instance, the energy density of a mechanical actuator is basically dependent on the strain that can be generated in its active materials. However, many other important performance indicators, such as the displacement, the force, actuation speed (or frequency) and energy efficiency will also depend on the material selection.

Spin crossover (SCO) complexes of $3d^4$–$3d^7$ transition metal ions are well known for changing a variety of physical properties during the transition between their high spin (HS) and low spin (LS) electronic configurations.[7,8] Despite copious investigations into their magnetic and optical properties, the spontaneous linear strain (ε) that can reach 8% (ref. 9 and 10) in these materials seems to be one of the most fascinating assets for practical applications.[11] The ε values in SCO complexes are high when compared to analogous phase transition materials. For example, in the very promising VO_2 known for the reversible metal–insulator phase change, a linear strain up to 2% can be reached.[12–16] Another important asset is that SCO can be provoked by different external stimuli such as temperature, pressure, magnetic field, excitation with light or adsorption of chemical species. The interest is additionally supported by the existence of hundreds of SCO complexes reported to date with different transition temperatures, hysteresis and abruptness of the spin transition.[7] This versatility can be further extended by the elaboration of composite materials. For example, SCO compounds have been imbedded in silica[17–19] and various polymer[20–25] matrices providing nanoscale confinement and/or better processability.

Recently we reported on the application of spin crossover materials for the elaboration of bimorph cantilevers, which were actuated both thermally and by light irradiation.[11] As a proof of concept, a single crystal of the SCO complex $\{Fe(3\text{-}CNpy)[Au(CN)_2]_2\}\cdot 2/3H_2O$ (py = pyridine) was covered with a layer of Al and used as a cantilever actuator. A reversible movement of this bimorph was reached as a result of thermally and photo-induced spin transitions, thus revealing a novel mechanism of actuation that opens up perspectives for the development of MEMS, artificial muscles and other applications for the harvesting and transformation of energy (thermal, electric, photonic, …). Additionally, three bilayer polymer/SCO

[a]LCC, CNRS & University of Toulouse (UPS, INPT), 205 route de Narbonne, 31077 Toulouse, France. E-mail: azzedine.bousseksou@lcc-toulouse.fr

[b]Department of Chemistry, Taras Shevchenko National University of Kyiv, 64 Volodymyrska Street, 01601 Kyiv, Ukraine

[c]LAAS, CNRS & Université de Toulouse (UPS, INSA, IAES), 7 avenue du colonel Roche, 31077 Toulouse, France

[d]Institut Carnot CIRIMAT, CNRS & Université de Toulouse III, 118 Route de Narbonne, 31062 Toulouse, France

[e]Department of Chemistry, University of Bath, Bath, BA2 7AY, UK. E-mail: h.j.shepherd@bath.ac.uk

† Electronic supplementary information (ESI) available: Actuation of a cantilever with a different geometry, detailed theoretical calculations, movie of the cantilever oscillation. See DOI: 10.1039/c4tc00267a

composite devices, each with different SCO compounds, were developed to demonstrate the versatility of SCO materials for actuating tasks. In this paper we go further by describing a prototype device that can exploit the spin transition phenomenon to convert electrical energy into motion *via* Joule heating in a composite bilayer actuator.

Results and discussion

SCO/polymer composites

Even though the application of a single crystal SCO material for the construction of bimorph cantilevers was found efficient and the behavior of these actuators is easy to rationalize from a theoretical point of view, the practical use of such systems has certain limitations. This is mostly related to the serendipity of the crystal growth. In contrast, techniques for employing polymers and polymer composites in MEMS design are well developed.[26] Hence, we synthesized a polymer composite material, consisting of the spin crossover complex $[Fe(trz)(H\text{-}trz)_2](BF_4)$ (form **1b**, one of the two forms described by Kröber *et al.*[27]) and the organic polymer PMMA, which can produce continuous films of several microns in thickness over a large area. This iron(II) compound is known for its abrupt and robust spin transition that takes place with a large thermal hysteresis around 85 °C on heating and 60 °C on cooling. It is important to note also that in this particular SCO complex the transition is accompanied by a volume change of 11%.[28]

A series of PMMA/**1b** composites with different relative proportions of the active complex were fabricated by mechanical dispersion of the powder of **1b** in a PMMA solution with subsequent evaporation of the chloroform solvent. A drop-casting procedure allows the deposition of the composite films over different surfaces. Films with different proportions (10–50%) of the active complex were produced (Fig. 1). Loading in excess of 50% of the SCO complex results in films that are brittle and cannot be removed from the substrate or further processed. The spin transition properties of these composites were observed and analyzed by optical microscopy since the SCO is accompanied by a drastic change of color in the active complex from pink in the LS state to colorless in the HS state. This effect is associated with the reversible bleaching of the characteristic $^1A_1 \rightarrow {}^1T_1$ absorption band centered around $\lambda = 550$ nm. Fig. 1 reveals a strong thermal dependence of the composite color that is clearly associated with the HS ↔ LS spin transition. The SCO in the composites takes place within the same region of temperature as for the pure complex. The transition curves of the composites were found to be relatively independent of the polymer/complex ratio; the most significant differences being a slight loss of abruptness of the spin transition for composites with lower loadings of the active material. This observation may simply be related to the lower thermal conductivity of the polymer component compared to the coordination compound. While the SCO behaviour of composite materials is in general not easy to predict, the negligible influence of a polymer matrix on those properties, as shown here, is certainly not unprecedented.[20–23]

Selected Raman spectra of $[Fe(trz)(H\text{-}trz)_2](BF_4)$ and the PMMA/$[Fe(trz)(H\text{-}trz)_2](BF_4)$ composite (50% loading) recorded at 20 °C and 110 °C are shown in Fig. 2. In the low frequency region (100–300 cm^{-1}), very significant changes are observed upon the SCO. As discussed in ref. 29, the modes at 300, 288, 211, 202 cm^{-1} are attributed to the LS state of the complex, whereas those at 186 and 109 cm^{-1} are associated with the HS state. These changes of the vibrational frequencies accompanying the spin transition are a general trend and originate from the strong electron–lattice coupling in these systems.[7] The disappearance of the characteristic LS/HS modes at high/low temperatures allows us to conclude that the spin transition is virtually complete in both directions for the isolated complex as well as for the composite material.

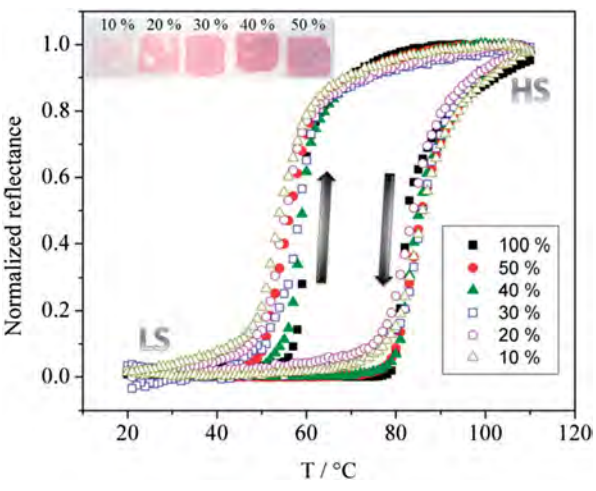

Fig. 1 Temperature dependence of the optical reflectance ($\lambda = 550$ nm) of $[Fe(trz)(H\text{-}trz)_2](BF_4)$ (100%) and of the composite materials PMMA/$[Fe(trz)(H\text{-}trz)_2](BF_4)$ with different loadings (10–50%) of the active complex. Heating and cooling modes are indicated by arrows. The inset shows the photographs of the composite films.

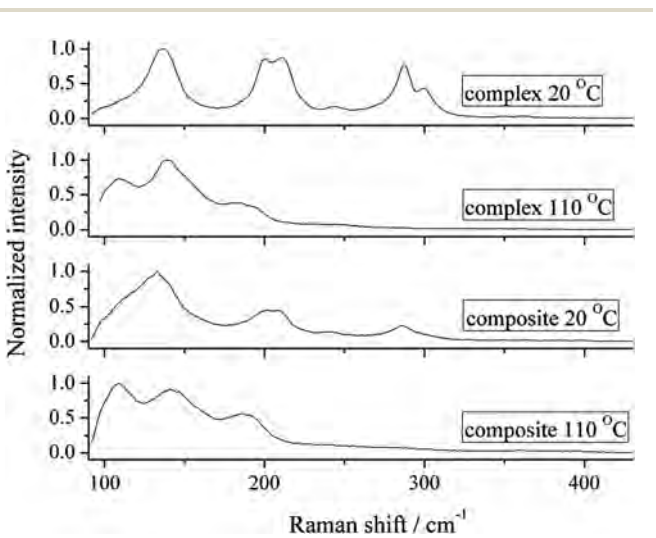

Fig. 2 Variable-temperature Raman spectra of the $[Fe(trz)(H\text{-}trz)_2](BF_4)$ complex and the PMMA/$[Fe(trz)(H\text{-}trz)_2](BF_4)$ (50%) composite material.

Differential scanning calorimetry (DSC) curves of $[Fe(trz)(H\text{-}trz)_2](BF_4)$ and the PMMA/$[Fe(trz)(H\text{-}trz)_2](BF_4)$ composite (50%) are shown in Fig. 3.

In agreement with the optical reflectivity and Raman spectroscopy measurements, these data demonstrate a high degree of similarity between the SCO in the isolated complex and the composite materials. Shifts of the transition temperatures between the complex and its composite are attributed to thermalization issues – an organic polymer would be expected to be less thermally conductive than a coordination compound. This measurement allows also the calculation of the enthalpy ($\Delta H =$ 25 kJ mol^{-1}) and entropy ($\Delta S = 73$ J mol^{-1} K^{-1}) changes associated with the spin transition in **1b**. These values were found similar for the isolated complex and the complex embedded in PMMA and they are also in good agreement with the data reported in ref. 27 for the pure complex.

Bilayer actuators

The composite film with the highest proportion of active material (50%) was then used to construct bilayer actuators. The highest possible loading by the active compound is expected to optimize the strain that can be transmitted from the complex to the polymer matrix, thus maximizing the actuating capabilities. Despite the proportion of the strain absorbed by the flexible polymer matrix, the spin transition in the active component results in a significant isotropic expansion of the composite material.

In a simple bilayer strip, the difference in expansion of the two layers results in the deflection of the cantilever that can be exploited for actuation. In our device, the second (inert) layer is used not only to generate the strain mismatch, but is also used as a heating element *via* the Joule effect. In such a way, the application of a current to the cantilever should provoke a spin transition (from LS to HS), while removing the current should cause a dissipation of heat followed by the reverse transition (HS to LS). We selected a polymer that was filled with silver particles (industrially available conductive paint) to act as the conductive layer because this conductive composite has a much higher adhesion to the active layer than a simple metal layer can have. Moreover, this choice for the conductive component makes both layers of the bimorph similar in terms of thermal expansion and Young's modulus. This minimizes the mismatch of the thermal expansion between the two layers and maximizes the deflection of the strip (for a given geometry).

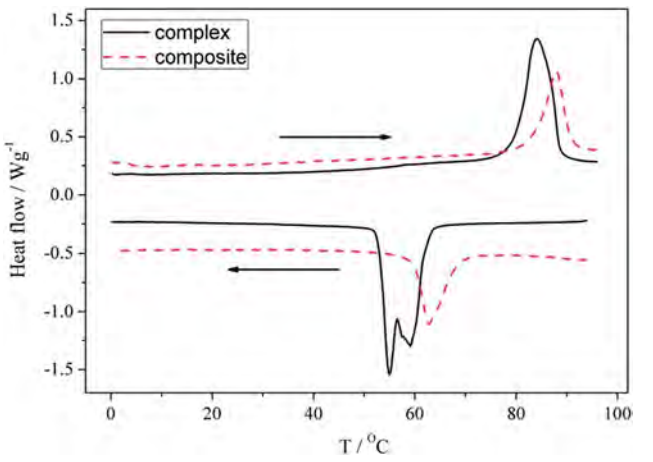

Fig. 3 DSC curves of the pure $[Fe(trz)(H\text{-}trz)_2](BF_4)$ complex and the PMMA/$[Fe(trz)(H\text{-}trz)_2](BF_4)$ (50%) composite material acquired at heating/cooling rates of 10 °C min^{-1}.

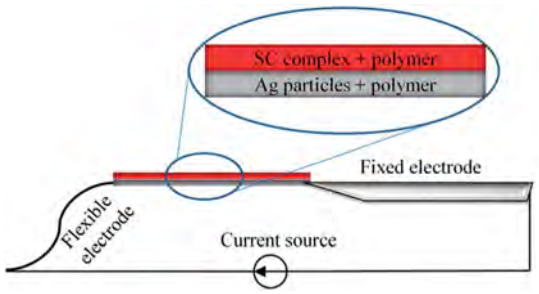

Fig. 4 Schematic representation of a SCO bilayer cantilever with electrothermal actuation.

The bilayer films were fabricated by spin-coating the conductive composite solution over a PMMA/SCO composite film. A cantilever was subsequently cut from this bilayer and connected to two electrodes: one electrode is fixed, whereas the second electrode is made of a flexible thin aluminium foil so as to allow (nearly) free movement with the cantilever (Fig. 4).

This setup was placed in a cryostat to control the temperature around the cantilever. The behavior of this cantilever was initially studied within a range of 23–100 °C. Heating was stopped at 100 °C to avoid any transformations of the polymers (*e.g.* glass transition) and damage of the device. As temperature increases the spin transition in $[Fe(trz)(H\text{-}trz)_2](BF_4)$ causes a spontaneous strain that results in a strong deformation of the bimorph at the temperature of the spin transition. The occurrence of SCO can also be clearly inferred from the simultaneous change of the composite color during the actuation (Fig. 5). The movement of the cantilever was quantified by following with a video-microscope the position of the end connected to the flexible electrode. Displacement as a function of temperature is shown in Fig. 5a.

The hysteresis loop of the thermal actuation (Fig. 5a) is rather deformed in comparison with the spin transition loop (Fig. 1). This is attributed to inefficient heat transfer from the heating plate to the cantilever suspended in air, attached only at the ends. In addition to heat exchange effects, mechanical stress can also influence the form of this curve. However, the limited region of temperature as well as the hysteretic nature of the deflection clearly demonstrate that tip deflection is the result of the spin transition in the active complex.

The amplitude of actuation (*ca.* 1600 μm) allows us to calculate the reactive force at the end of the cantilever and the effective linear strain of the composite material to be ~20 mN and ~1%, respectively (see ESI† for details on the calculations). These values are slightly underestimated since the flexible electrode acts as a load on the cantilever. Nevertheless the

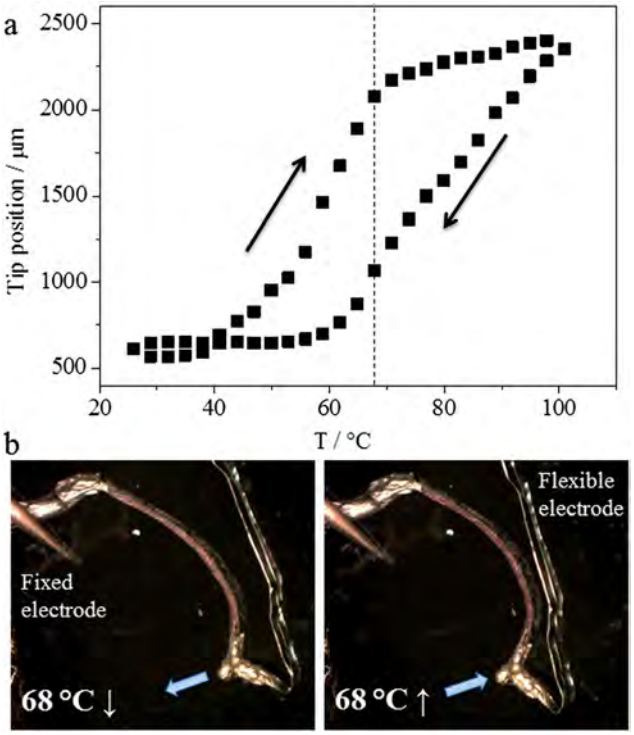

Fig. 5 Thermal actuation of a bimorph cantilever. (a) Tip position of the cantilever as a function of temperature. Heating and cooling modes are indicated by arrows. (b) Photographs (8.6 mm × 7.6 mm) of the cantilever at 68 °C in the cooling and heating modes demonstrate a shape memory effect, which occurs due to the thermal hysteresis of the spin transition. The color change associated with the spin transition is also observed (see also ESI Movie SM1†).

effective strain is significantly lower than that estimated from the additive effect (*ca.* 2%), which we relate to the partial absorption of strain by the polymeric matrix. The efficiency of this material for actuation is described by the volumetric work density W/V, *i.e.* the maximal mechanical output, which can be produced by a given volume of the composite. W/V for the 50% composite was calculated to be *ca.* 150 mJ cm^{-3} (see ESI† for details on the calculations). This value is comparable or higher than those reported for piezo-electric, magnetostrictive and electroactive polymer materials.[30]

Electrothermal actuation of the cantilever

To generate an electrothermally driven actuation, a squared current (I) was applied to the cantilever, which engenders Joule heating. In a typical experiment, I was changed stepwise from 0 to I_{max} and back to 0 at a constant frequency (f). When $I = I_{max}$, the LS → HS transition is induced, whereas removing the current leads to the backward HS → LS transition. This sequence of LS → HS → LS transitions provokes oscillating motion of the cantilever (Fig. 6). The amplitude of this movement is constant in numerous cycles (see also ESI Movie SM1†). In this experiment, the device was passed through more than 300 actuating cycles with no observed fatigue of the actuator. It is worth noting that though the flexible electrode acts as an

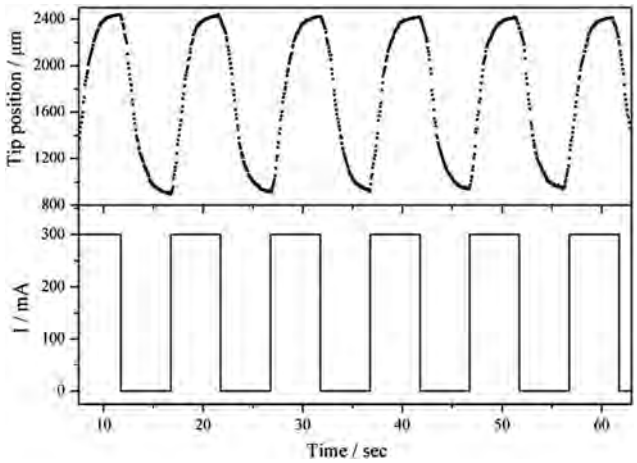

Fig. 6 Electric current induced actuation of a bimorph cantilever. Tip position of the cantilever as a function of time (upper panel) and the corresponding applied current signal (bottom panel). The frequency of the alternative current is 0.1 Hz, $I_{max} = 300$ mA, $T = 20$ °C.

additional load, it does not play a crucial role in the movement of the cantilever. This is due to the force (~20 mN) generated at the tip of the cantilever being considerably higher than the force necessary to move the aluminium foil.

After an initial "run-in" period of a few cycles, the actuating amplitude becomes highly repeatable within the given operating conditions (Fig. 6). We observed that this amplitude depends strongly on the experimental conditions. The most important contributing factor is the fraction of the complex that undergoes SCO when the current is turned on/off. This leads to different amplitudes of deflection with different applied frequency, current and temperature of the surrounding medium. A series of experiments were designed to probe the interdependence of these three parameters (I_{max}, f and T).

The amplitude of cantilever movement is shown as a function of applied current in Fig. 7. A current below 200 mA does

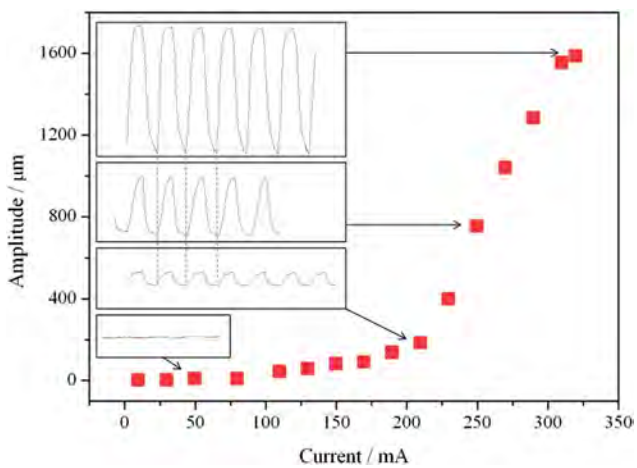

Fig. 7 Amplitude of oscillation of the bilayer cantilever as a function of the applied current I_{max} at constant temperature and frequency ($T = 20$ °C, $f = 0.1$ Hz). Insets: tip position of the cantilever as a function of time for a few selected values of I_{max}.

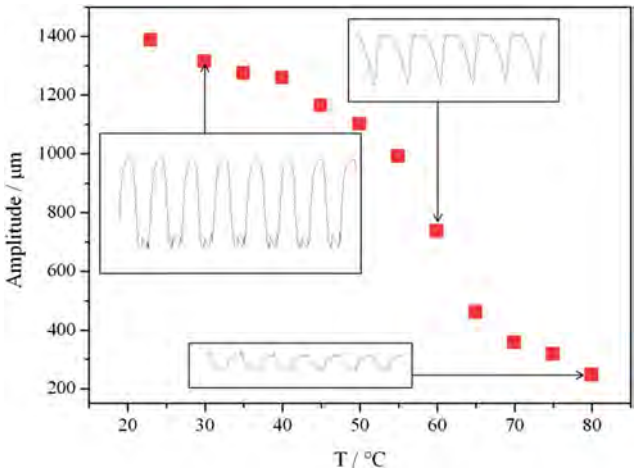

Fig. 8 Amplitude of the bilayer cantilever oscillation at different temperatures. The ac current and frequency were fixed (I_{max} = 300 mA, f = 0.1 Hz). Insets: tip position of the cantilever as a function of time at selected temperatures.

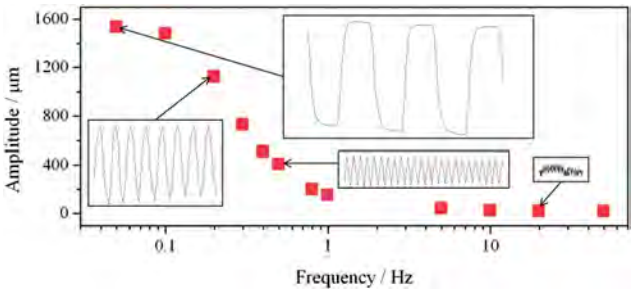

Fig. 9 Amplitude of the bilayer strip oscillation as a function of frequency at constant temperature and ac current (T = 20 °C, I_{max} = 300 mA). Insets: tip position of the cantilever as a function of time at selected frequencies.

not result in any significant actuation of the cantilever. This threshold effect is likely to be the result of insufficient heating, *i.e.* below a certain temperature the nucleation of the HS phase cannot take place. The low amplitude oscillation observed for currents below this value should be considered chiefly as a thermal expansion effect without SCO. By contrast, a current over 200 mA generates enough heat to induce the thermal SCO, reaching a maximum amplitude of actuation at $I_{max} \approx 300$ mA. The deflection at currents between 200 and 300 mA corresponds to a partial spin transition of the Fe(II) complex in the composite. This threshold current value can be tuned *via* several different approaches, including the change of SCO active complex. Indeed, the use of any SCO compound with higher/lower temperature of transition should increase/decrease the critical value of current necessary to drive the cantilever oscillation.

Measurements at constant f and I_{max} reveal a clear dependence of the actuation amplitude on the surrounding temperature as shown in Fig. 8. Up to 50 °C a slight and almost linear diminution of the actuating amplitude is observed and can be explained by an incomplete HS to LS transition when the current is switched off. Above 50 °C an abrupt drop off in amplitude is observed, due to the thermal SCO occurring above this point. Thus, even when there is no current applied to the cantilever, a significant fraction of the active SCO complex remains in the HS state.

Again, this characteristic cut-off temperature can be tuned by substituting the active complex for another SCO material. The abrupt on/off switch of the actuation with temperature can be achieved by using highly cooperative spin crossover systems where the spin state change occurs sharply within < 1 K. (*N.B.* To observe an abrupt cut-off as a function of temperature efficient thermalization is also necessary.) On the other hand, the use of compounds with a gradual SCO – taking place within hundreds degrees – can allow fine control over the actuation amplitude by changing the environmental temperature.

Varying the frequency at constant I_{max} and T reveals a cut-off of the actuation (defined as a decay in amplitude of 0.707 of the maximum value) at $f_{cut\ off} \approx 0.5$ Hz (Fig. 9). In this case the completeness of the transition in both directions (LS to HS and HS to LS) is limited by the rate of heat diffusion; there is insufficient time for the device to reach the required temperature to switch all active centers. For this actuator there is no frequency limitation up to f = 0.1 Hz; however, no movement is observed for f > 1 Hz. This limitation is clearly related to the heat transfer processes and not to the spin conversion process that has much faster dynamics.[7,8]

The observed cut-off frequency is not a fundamental limit, but rather denotes that (if necessary) the device must be operated at a different temperature and/or a different current should be applied. Even more importantly, the cantilever geometry and the thermalisation conditions can also drastically change the performance of these actuators in terms of actuating speed. One example describing the effect of a different geometry is shown in the ESI (Fig. S1–S3†). A cantilever of a smaller size was fabricated and studied in a similar manner. A direct consequence of the size reduction is the faster heat exchange between the cantilever and its surroundings. Thus, a lower cut-off temperature and current, as well as a higher cut-off frequency were observed.

Experimental information

PMMA (M_w = 550 000), iron(II) tetrafluoroborate hexahydrate, 1-*H*-1,2,4-triazole and chloroform were purchased from Sigma Aldrich and used without any further purification. Conductive silver paint RS 186-3593 was purchased from RS Components. This paint contains a polymeric basis filled with silver microspheres (<18 μm, 56%) and dissolved in an *n*-butyl acetate/2-methoxy-1-methylethyl acetate mixture.

$[Fe(trz)(H\text{-}trz)_2](BF_4)$ (form **1b**) was prepared from $Fe(BF_4)_2 \cdot 6H_2O$ and 1-*H*-1,2,4-triazole according to the procedure described by Kröber *et al.*[27] The active composite material was elaborated by mechanical dispersion of the $[Fe(trz)(H\text{-}trz)_2](BF_4)$ powder (5 mg) in a solution of PMMA (5 mg) in $CHCl_3$ (200 μl). This suspension was drop-casted onto a silicon substrate (1 × 1 cm^2) and allowed to dry. 150 μl of the conductive paint was subsequently spin coated (2000 rpm, 3000 rpss, 30 s) onto the upper surface. The resulting bilayer film was removed from the substrate and cut into cantilevers. The cantilever used was 6.7

mm in length and 1 mm in width. The thicknesses of the SCO and conductive layers were *ca.* 100 and 50 μm, respectively.

Variable temperature Raman spectra of the samples were acquired by means of an Xplora (Horiba) microspectrometer and a Linkam THMS600 cryostat. A long working-distance objective (×50, numerical aperture = 0.5) was used to focus the laser beam (638 nm, 0.1 mW) on the sample and to collect the scattered photons. Rayleigh scattering was removed by an edge filter. Differential scanning calorimetry analysis was carried out on a Netsch DSC 204 instrument under helium purging gas. The measurements were conducted between 0 and 100 °C at a scan rate of 10 K min^{-1} both on heating and cooling. Temperature and enthalpy were calibrated using the melting transition of standard materials (Hg, In, Sn).

In order to perform the electrical actuation experiments, a cantilever was fixed onto a fixed steel electrode with the conductive paint. The other side was attached to a flexible aluminium electrode (10 μm thick) in the same manner. The temperature was controlled using a Linkam HFS600E cryostat equipped with flexible internal microelectrodes to connect the device to the current source. The videomicroscopy and optical reflectivity images were acquired with a MOTIC stereomicroscope equipped with a colour camera. Current pulses were generated with a programmable current source (Keithley 6430). Tip displacement was determined from the video images. The image treatments were carried out under ImageJ and MatLab environments as described previously.[11]

Conclusions and perspectives

The spin crossover complex $[Fe(trz)(H\text{-}trz)_2](BF_4)$ was dispersed in an organic polymer matrix to form freestanding films. The spin crossover properties of the isolated complex were preserved in the composites, which allowed us the development of a highly efficient electromechanical actuating device with a volumetric work density of *ca.* 150 mJ cm^{-3}. The prototype device described here exhibited repeatable and tunable actuation *via* temperature, frequency and current variation and provided both large force (several mN) and large displacement (several mm). The procedure to elaborate the active composites can be easily extended not only to other SCO compounds, but also to different phase transition materials (VO_2, *etc.*). This approach of actuation driven by SCO can be also introduced in MEMS/NEMS sensors, since several SCO compounds have shown a good sensitivity to different hazardous compounds.[31] An exciting perspective of this work will be the investigation of the effects of scaling, since the faster heat transfer rate at reduced scales will result in higher work frequency and effectiveness.[5] This prospect is tangible since the spin transition properties can be preserved down to very small sizes.[8]

Acknowledgements

Financial support from the project Switchelec (ANR-12-IS07-0003-01) is acknowledged. JSC thanks the Marie-Curie research program (NanoSCOpe 328078).

Notes and references

1 M. Bao, in *Analysis and Design Principles of MEMS Devices*, Elsevier Science, Amsterdam, 2005, pp. 1–32.
2 *Comprehensive Microsystems*, ed. Y. Gianchandani, O. Tabata and H. Zappe, Elsevier, Oxford, 2008, vol. 2, pp. 1–100.
3 T.-L. Ren, H.-J. Zhao, L.-T. Liu and Z.-J. Li, *Mater. Sci. Eng., B*, 2003, **99**, 159–163.
4 S. Pal and H. Xie, *J. Micromech. Microeng.*, 2012, **22**, 115036.
5 P. Srinivasan and S. M. Spearing, *J. Microelectromech. Syst.*, 2008, **17**, 653–667.
6 *MEMS Materials and Processes Handbook*, ed. R. Ghodssi and P. Lin, Springer US, Boston, MA, 2011, vol. 1.
7 *Spin Crossover in Transition Metal Compounds, Top. Curr. Chem.*, ed. P. Gütlich and H. A. Goodwin, Springer, Berlin, Heidelberg, 2004, vol. 233–235.
8 A. Bousseksou, G. Molnár, L. Salmon and W. Nicolazzi, *Chem. Soc. Rev.*, 2011, **40**, 3313–3335.
9 P. Guionneau, *Dalton Trans.*, 2014, **43**, 382–393.
10 S. Cobo, D. Ostrovskii, S. Bonhommeau, L. Vendier, G. Molnár, L. Salmon, K. Tanaka and A. Bousseksou, *J. Am. Chem. Soc.*, 2008, **130**, 9019–9024.
11 H. J. Shepherd, I. A. Gural'skiy, C. M. Quintero, S. Tricard, L. Salmon, G. Molnár and A. Bousseksou, *Nat. Commun.*, 2013, **4**, 2607.
12 R. Cabrera, E. Merced, N. Sepúlveda and F. E. Fernández, *J. Appl. Phys.*, 2011, **110**, 094510.
13 J. Cao, W. Fan, Q. Zhou, E. Sheu, A. Liu, C. Barrett and J. Wu, *J. Appl. Phys.*, 2010, **108**, 083538.
14 K. Liu, C. Cheng, Z. Cheng, K. Wang, R. Ramesh and J. Wu, *Nano Lett.*, 2012, **12**, 6302–6308.
15 A. Rúa, F. E. Fernández and N. Sepúlveda, *J. Appl. Phys.*, 2010, **107**, 074506.
16 K. Wang, C. Cheng, E. Cardona, J. Guan, K. Liu and J. Wu, *ACS Nano*, 2013, **7**, 2266–2272.
17 C. Faulmann, J. Chahine, I. Malfant, D. de Caro, B. Cormary and L. Valade, *Dalton Trans.*, 2011, **40**, 2480–2485.
18 S. Titos-Padilla, J. M. Herrera, X.-W. Chen, J. J. Delgado and E. Colacio, *Angew. Chem., Int. Ed.*, 2011, **50**, 3290–3293.
19 P. Durand, S. Pillet, E.-E. Bendeif, C. Carteret, M. Bouazaoui, H. El Hamzaoui, B. Capoen, L. Salmon, S. Hebert, J. Ghanbaja, L. Arandah and D. Schaniel, *J. Mater. Chem. C*, 2013, **1**, 1933–1942.
20 S.-W. Lee, J.-W. Lee, S.-H. Jeong, I.-W. Park, Y.-M. Kim and J.-I. Jin, *Synth. Met.*, 2004, **142**, 243–249.
21 A. Nakamoto, Y. Ono, N. Kojima, D. Matsumura and T. Yokoyama, *Chem. Lett.*, 2003, **32**, 336–337.
22 M.-L. Boillot, S. Pillet, A. Tissot, E. Rivière, N. Claiser and C. Lecomte, *Inorg. Chem.*, 2009, **48**, 4729–4736.
23 M. Rubio, R. Hernandez, A. Nogales, A. Roig and D. Lopez, *Eur. Polym. J.*, 2011, **47**, 52–60.
24 J. Larionova, L. Salmon, Y. Guari, A. Tokarev, K. Molvinger, G. Molnár and A. Bousseksou, *Angew. Chem., Int. Ed.*, 2008, **47**, 8236–8240.
25 W. Hellel, A. Ould-Hamouda, J. Degert, J.-F. Létard and E. Freysz, *Appl. Phys. Lett.*, 2013, **103**, 143304.

26 C. Liu, *Adv. Mater.*, 2007, **19**, 3783–3790.
27 J. Kröber, J.-P. Audiere, R. Claude, E. Codjovi, O. Kahn, J. G. Haasnoot, F. Groliere, C. Jay and A. Bousseksou, *Chem. Mater.*, 1994, **6**, 1404–1412.
28 A. Grosjean, P. Négrier, P. Bordet, C. Etrillard, D. Mondieig, S. Pechev, E. Lebraud, J.-F. Létard and P. Guionneau, *Eur. J. Inorg. Chem.*, 2013, 796–802.
29 N. O. Moussa, D. Ostrovskii, V. M. Garcia, G. Molnár, K. Tanaka, A. B. Gaspar, J. A. Real and A. Bousseksou, *Chem. Phys. Lett.*, 2009, **477**, 156–159.
30 V. Q. Nguyen, A. S. Ahmed and R. V. Ramanujan, *Adv. Mater.*, 2012, **24**, 4041–4054.
31 C. Bartual-Murgui, A. Akou, L. Salmon, G. Molnár, C. Thibault, J. A. Real and A. Bousseksou, *Small*, 2011, **7**, 3385–3391.